Electronic Supplementary Information (ESI)

Stepwise synthesis of CoS_2-C@CoS_2 yolk-shell nanocages with much enhanced electrocatalytic performances both in solar cells and hydrogen evolution reactions

Yudi Niu, Xing Qian,* Jie Zhang, Weimin Wu, Hongyu Liu, Chong Xu and Linxi Hou*

College of Chemical Engineering, Fuzhou University, Xueyuan Road No. 2, Fuzhou 350116, China. *E-mails: xingqian@fzu.edu.cn; lxhou@fzu.edu.cn.
Fax: +86-0591-2286 6244; Tel: +86-0591-2286 5220.

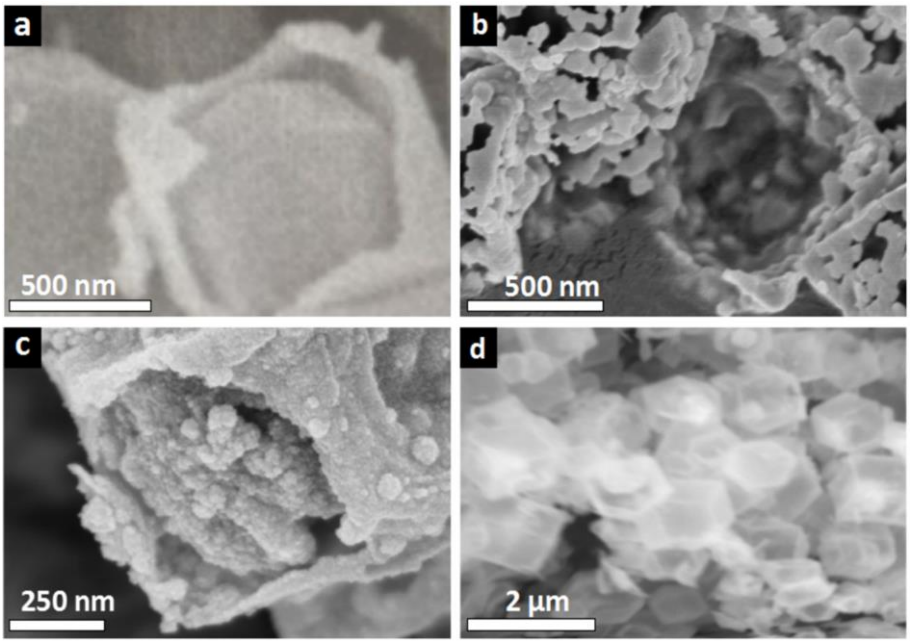

Fig. S1. SEM images of the cracked (a) CoS-C@CoS, (b) CoS/CoS_2-C, (c) CoS_2-C@CoS_2 after ultrasonic treatment, and (d) tungsten light scanning electron microscopy (TLSEM) image of CoS-C@CoS.

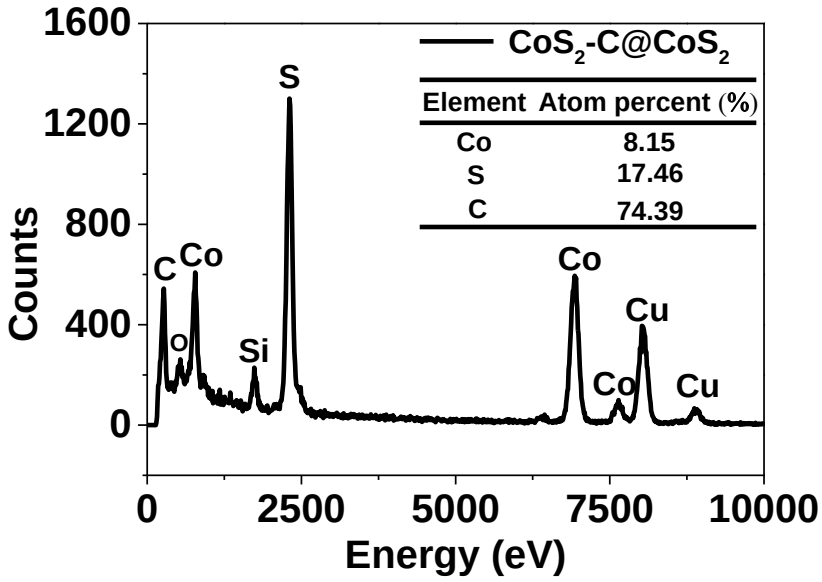

Fig. S2. EDX spectra image of CoS_2-C@CoS_2.

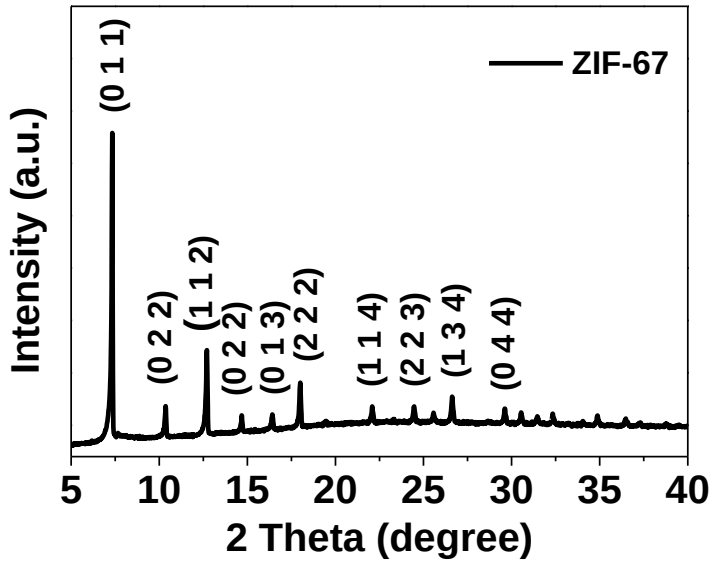

Fig. S3. XRD spectra of ZIF-67.

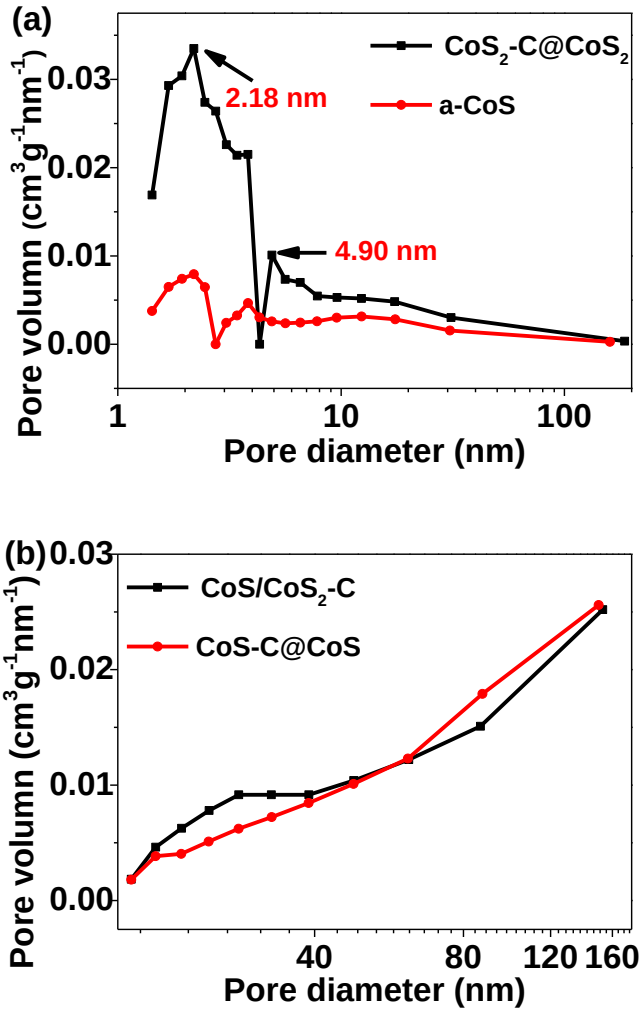

Fig. S4. Pore-size distribution of CoS_2-C@CoS_2, a-CoS, CoS/CoS_2-C and CoS-C@CoS.

Table S1. Pore-structure parameters derived from the BET curves.

Samples	Pore volume($cm^3\ g^{-1}$)	Specific area ($m^2\ g^{-1}$)
CoS_2-C@CoS_2	0.322	161
CoS/CoS_2-C	0.109	13.9
CoS-C@CoS	0.081	12.3
a-CoS	0.153	43.9

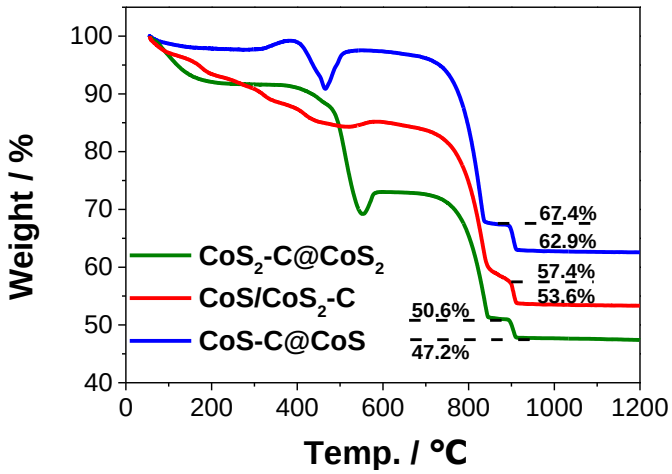

Fig. S5. Thermogravimetric (TGA) curves of CoS_2-C@CoS_2, CoS/CoS_2-C and CoS-C@CoS samples.

Thermogravimetric analysis (TGA) of these samples was performed in air atmosphere to investigate the compositions of CoS_2-C@CoS_2, CoS/CoS_2-C and CoS-C@CoS (Figure S5, ESI). A weight loss below 200 °C was measured for the samples, which was ascribed to the disappearance of adsorbed water. The observed weight loss between 200 and 500 °C was mainly attributed to the combustion of the C element.[1] An increase in weight, followed by a decrease in weight, which was observed between 500 and 735 °C, was ascribed to an initial oxidation of CoS_2/CoS transforming to $CoSO_4$. Then, the subsequent decomposition of $CoSO_4$ transformed to Co_3O_4 between 735 °C and 890 °C. During this temperature, the mass content of the residual Co_3O_4 of the samples CoS_2-C@CoS_2, CoS/CoS_2-C and CoS-C@CoS was 50.6%, 57.4% and 67.4%, respectively. At the end, the stable mass content of CoO which was transformed by Co_3O_4 from 890 to 910 °C has been recorded as 47.2%, 53.6% and 62.9%, respectively. By calculations, the roughly estimated mass loading of CoS_2/CoS in CoS_2-C@CoS_2, CoS/CoS_2-C (the main component can be observed as CoS_2, according to the XRD result) and CoS-C@CoS were 77.4%, 87.9% and 76.3%, respectively.

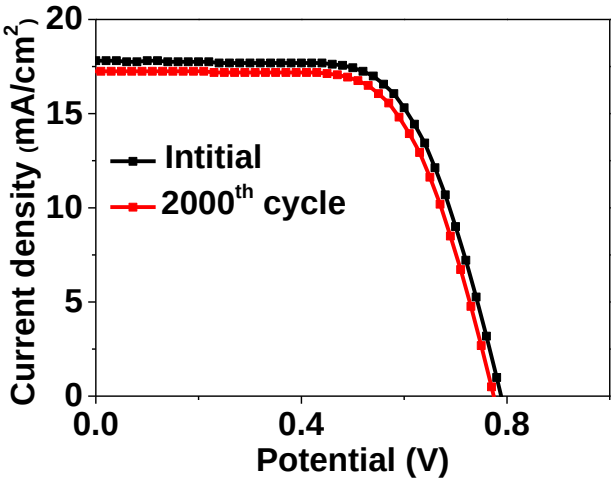

Fig. S6. *J*−*V* curves of CoS_2-C@CoS_2 before and after 2000 times CV cycles.

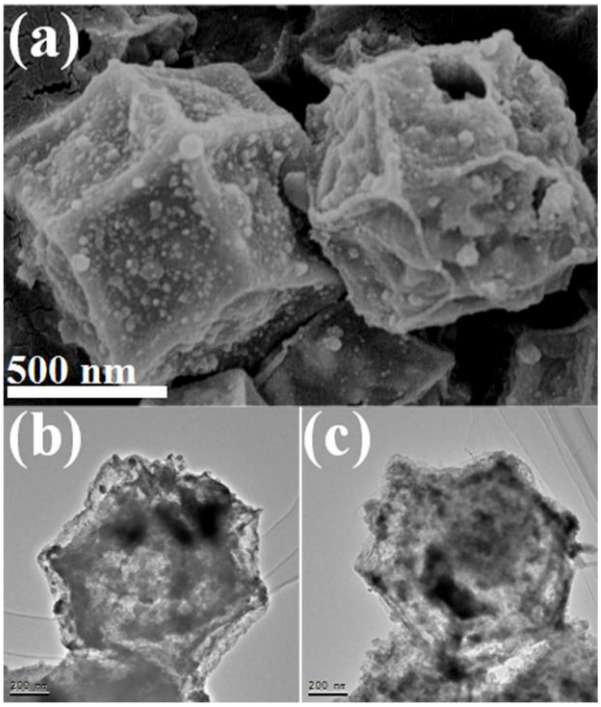

Fig. S7. (a) SEM image and (b, c) TEM images of CoS_2-C@CoS_2 after the HER test.

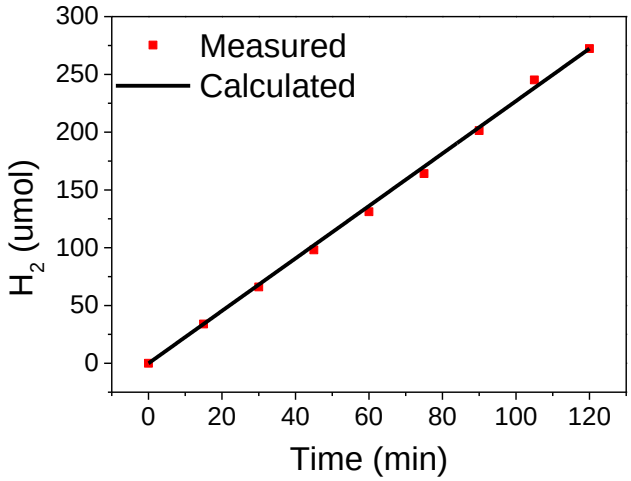

Fig. S8. Calculated (solid line) and measured (red dot) amount of hydrogen at different times for CoS_2-C@CoS_2 at a constant current density of 20 mA cm^{-2} in 0.5 M H_2SO_4.

Table S2. Comparisons of DSSC performances for as-obtained samples with other non-noble metal-based catalysts.

catalyst	η (%)	η_{Pt} (%)	η/η_{Pt}	References
CoS_2-C@CoS_2	9.32	8.24	1.13	This work
MOF-525/s-PT	8.91	8.21	1.08	2
CoS_2-C	8.20	7.88	1.04	3
$CoNi_2S_4$ nanoribbon-CF	7.03	6.45	1.09	4
CoS_2/RGO	7.69	7.38	1.04	5
CoS_2	6.13	6.04	1.01	6
CSG	5.43	5.84	0.93	7
$CoSe_2$/C-NCW	8.92	8.25	1.08	8
$CoSe_2$	8.38	7.83	1.07	9
$NiCo_2S_4$ nanosheet	7.22	6.89	1.04	10
$CoNi_2S_4$ nanosheet	3.72	4.67	0.80	11

Table S3. Comparison of HER performance in acidic medium for as-obtained samples with other non-noble metal-based catalysts.

Catalysts	Onset potential (mV)	η_{10} (mV)	Tafel slope (mV decade^{-1})	References
CoS_2-C@CoS_2	19.0	79.1	51.9	This work
CoS_2-MW	—	158	58.0	12
Co_9S_8/CNFs	—	186	83	13
CoP/CNs	55	135	58	14
CoMoS/$CoMoO_4$	80	—	58	15
Co-CN	181	266	112	16
CoP NPs	—	100	~60	17
CoP CPHs	—	133	51	18
MoS_2/Co_3S_4	—	175	55.6	19
NPPC	51	159	74	20

References

1 S. Huang, Y. Meng, S. He, A. Goswami, Q. Wu, J. Li, S. Tong, T. Asefa and M. Wu, *Adv. Funct. Mater.*, 2017, **27**, 1606585.

2 T. Y. Chen, Y. J. Huang, C. T. Li, C. W. Kung, R. Vittal and K. C. Ho, *Nano Energy*, 2017, **32**, 19–27.

3 X. D. Cui, Z. Q. Xie and Y. Wang, *Nanoscale*, 2016, **8**, 11984−11992.

4 L. Chen, Y. Zhou, H. Dai, T. Yu, J. G. Liu and Z. G. Zou, *Nano Energy*, 2015, **11**, 697–703.

5 H. Yuan, J. Liu, Q. Jiao, Y. Li, X. Liu, D. Shi, Q. Wu, Y. Zhao and H. Li, *Carbon*, 2017, **119**, 225–234.

6 J. C. Tsai, M. H. Hon and I. C. Leu, *Chem. - Asian J.*, 2015, **10**, 1932–1939.

7 L. Sun, Y. Bai, N. Zhang and K. Sun, *Chem. Commun.*, 2015, **51**, 1846–1849.

8 I. T. Chiu, C. T. Li, C. P. Lee, P. Y. Chen, Y. H. Tseng, R. Vittal and K. C. Ho, *Nano Energy*, 2016, **22**, 594–606.

9 J. Dong, J. Wu, J. Jia, S. Wu, P. Zhou, Y. Tu and Z. Lan, *Electrochim. Acta*, 2015, **168**, 69–75.

10 S. Y. Khoo, J. Miao, H. B. Yang, Z. He, K. C. Leong, B. Liu and T. Y. Tan, *Adv. Mater. Interfaces*, 2015, **2**, 1500384.

11 Z. Shi, K. Deng and L. Li, *Sci. Rep.*, 2015, **5**, 9317.

12 M. S. Faber, R. Dziedzic, M. A. Lukowski, N. S. Kaiser, Q. Ding and S. Jin, *J. Am. Chem. Soc.*, 2014, **136**, 10053−10061.

13 L. Gu, H. Zhu, D. Yu, S. Zhang, J. Chen, J. Wang, M. Wan, M. Zhang and M. Du, *Part. Part. Syst. Charact.*, 2017, **34**, 1700189.

14 T. Li, D. Tang and C. Li, *Int. J. Hydrogen Energy*, 2017, **42**, 21786−21792.

15 Y. R. Liu, X. Shang, W. K. Gao, B. Dong, X. Li, X. H. Li, J. C. Zhao, Y. M. Chai, Y. Q. Liu and C. G. Liu, *J. Mater. Chem. A*, 2017, **5**, 2885−2896.

16 J. Chen, H. Zhou, Y. Huang, H. Yu, F. Huang, F. Zheng and S. Li, *RSC Adv.*, 2016, **6**, 42014−42018.

17 D. H. Ha, B. Han, M. Risch, L. Giordano, K. P. C. Yao, P. Karayaylali and Y. Shao-Horn, *Nano Energy*, 2016, **29**, 37−45.

18 M. Xu, L. Han, Y. Han, Y. Yu, J. Zhai and S. Dong, *J. Mater. Chem. A*, 2015, **3**, 21471−21477.

19 X. Lei, K. Yu, H. Li and Z. Zhu, *Electrochim. Acta*, 2018, **269**, 262−273.

20 Y. Lin, J. Zhang, Y. Pan and Y. Liu, *Appl. Surf. Sci.*, 2017, **422**, 828−837.